

In Silico Screening for Novel Anti-COVID Phytochemicals from the Rhizome of *Curcuma longa*

Timothy P. C. Ezeorba ^{1,2,*}, Nene O. Uchendu ¹, Ekene J. Nweze ¹, Chibuzo K. Okoroafor ¹, Pascal O. Ogbu ¹, Miracle C. Okpara ¹, Rita O. Asomadu ¹ and Parker E. Joshua ^{1*}

¹ Department of Biochemistry, Faculty of Biological Sciences, University of Nigeria, Nsukka

² Department of Molecular Biotechnology, School of Biosciences, University of Birmingham, Edgbaston Birmingham B15 2TT United Kingdom

* Correspondence: timothy.ezeorba@unn.edu.ng (T.P.C.E.); parker.joshua@unn.edu.ng (P.E.J.); Tel.: +234 813 9394 632 (T.P.C.E)

† Presented at the 1st International Electronic Conference on Molecular Sciences: Druggable Targets of Emerging Infectious Diseases, online, 01-14 September 2021.

Academic Editor: Clemente Capasso

Published: 31 August 2021

Abstract: The devastating nature of the SARS-CoV-2 pandemic has fostered the need for potent therapeutics to manage or curb its severity. As a response, several studies on drug repurposing, vaccine design and optimizing natural phytochemicals are ongoing. This study aims at screening for potent and novel anti-COVID phytochemicals from the rhizome of *Curcuma longa*. A phytochemical library of 50 non-ubiquitous bioactive compounds from the rhizome of *Curcuma longa* was retrieved from Dr. Duke's phytochemical and ethnobotanical database (<https://phytochem.nal.usda.gov/phytochem/search>). The compounds in the library were docked against the receptor binding domain (RBD) of SARS-CoV-2 (PDB ID: 7EAM_1). Three compounds - Quercetin; 1,7-Bis-(4-hydroxyphenyl)-1-heptene-3,5-dione; and Cyclocurcumin, were selected based on their higher docking score than the standard repurposed drug (Arbidol). This study further examined the interactions of the novel 1,7-Bis-(4-hydroxyphenyl)-1-heptene-3,5-dione (BHHD) in the binding pocket as well as its ADMET properties. Excellent interaction was observed between the atoms of BHHD and amino acid residues known to foster the viral entry into the host. Furthermore, the ADMET result for BHHD was impressive for a lead molecule. Therefore, this study recommends for further investigation on the potency and toxicity of BHHD both on cell lines and animal models.

Keywords: SARS-CoV-2; Anti-COVID; ADMET; 1,7-Bis-(4-hydroxyphenyl)-1-heptene-3,5-dione (BHHD), Molecular Docking;

1. Introduction

Coronaviruses are distinct classes of viruses that infect animals, including humans. They are characterized with respect to the disease and associative-symptoms they cause [1]. The WHO recently declared a global pandemic of a new coronavirus disease 2019 (COVID-19) due to the invasiveness of the novel coronavirus - Severe Acute Respiratory Syndrome Coronavirus 2 (SARS-CoV-2) [2]. Since its first outbreak in Wuhan, Hubei province of China, as of December 2019, Sars-CoV-2 has continued to spread worldwide, infecting millions of individuals and causing several hundreds of thousands of deaths [3]. Due to the devastating nature of this disease and lack of required medications, already existing drugs with a supposed potential for treating Coronavirus disease-2019 (COVID-19) has been utilized as a better alternative [4].

Reviews have suggested an effective role of phytochemicals in fighting against viral diseases. In the last two decades, phytochemicals have been proven effective against viral outbreaks of the same family of Coronavirus [SARS-CoV (2003) and MERS-CoV (2012)] [5]. Likewise, at the onset of COVID-19, it was suggested that phytochemicals would be a potential candidate for its treatment and prevention (attia *et al.*, 2020). Plants such as turmeric, garlic, ginger and bitter kola are examples of such plants whose phytochemicals were suggested to provide benefits in a variety of viral illnesses (Attah *et al.*, 2021).

In this study, the anti-COVID phytochemicals from the rhizome of *Curcuma longa* (RCL) were screened out using extra precision GLIDE package (XP-GLIDE) of the Schrodinger suite.

2. Materials and Methods

2.1. Materials

A computer workstation with 4 core, 8 Gigabyte RAM and 2.5 GHz processor speeds

2.2. Methods

2.2.1. Formulation of the Ligand Library

The ligand library was generated from the collation of non-ubiquitous bioactive phytochemicals from the rhizome of *Curcuma longa* retrieved from Dr. Duke's Phytochemical and Ethnobotanical Databases (<https://phytochem.nal.usda.gov/phytochem/search>). The phytochemical 2D structures collated in a .csv file was obtained from PubChem database (<https://pubchem.ncbi.nlm.nih.gov/>) and processed into its 3D energy-minimized structures using the LigPrep package of Schrodinger Suite v20.03.

2.2.2. Retrieval of Structure of SARS-CoV-2 Spike protein

The x-ray crystal structure of the spike protein for SARS-CoV-2 was retrieved from the Protein Data Bank (<https://www.rcsb.org/>). Out of the 447 structure of the SARS-CoV-2 glycoprotein, the structure with the PDB ID of 7EAM_1 (Spike Protein) was selected for this study because of its high resolution of 1.4 Å from X-ray crystallization experiment. The quality of the protein structure was further ascertained with the Structure Analysis Package of Schrodinger Suite v20.03

2.2.3. Preparation of Retrieved Protein

The preparation of the Spike protein (7EAM_1) for molecular docking was performed on the Protein Preparation Wizard of the Schrodinger Suite v20.03. To prepare the protein structure, all atoms were assigned a bond order, missing hydrogen from the X-ray crystallized structure was added, all the non-interacting water molecules removed, energy minimized disulfide bonds were created, missing side chains and loops were modeled with primed and energy minimized in an OPLS3e force field. The Ramachandran plot protein reliability report was generated to estimate the quality of the protein structure after protein preparation process.

2.2.4. Prediction of Binding Site and Generation of Grid for Docking

The probable binding site for the protein was predicted using a sitemap tool in Schrodinger suite v20.03. The binding pocket with the best site score and deepest volume was selected for the studies. Using the Receptor Grid Generation Package, a grid was generated around the premise of the selected binding site, which was then used for molecular docking experiments.

2.2.5. Protein Ligand Molecular Docking

The molecular docking of the library of phytochemicals from *Curcuma longa* to the RBD domain of the spike protein of SARS-CoV-2 was performed with Standard Precision

module of the Grid Ligand Docking with Energy Package (SP-GLIDE). The top five ligands based on their docking score and glide score were selected for re-docking with the Extra-Precision Grid Ligand Docking with Energy Package (XP-GLIDE) under the optimized force field of OPLS3e. The relative interaction with the ligand in the binding pocket of the protein was studied in the XP- visualizer and the pictorial representation in 2D and 3D was generated.

2.2.5.1. Docking a Standard Repurposed Drug for Spike Protein

Out of 15 known repurposed drugs for SARS-COV-2, Arbidol (CID: 131411) was selected as the standard drug for this study because of the direct mechanism of action on the RBD domain of the spike protein. Arbidol was docked to SARS-CoV-2 receptor binding domain (7EAM_1) using XP-GLIDE and used as a standard reference to compare the efficacy of the top selected ligand from the library.

2.2.5.2. Prediction of the ADMET properties

The adsorption, distribution, metabolism, excretion and toxicity (ADMET) properties of the top selected ligand from the library was analyzed on the SwissADME free open access web server (<http://www.swissadme.ch/>). The physiochemical properties, Lipophilicity, water solubility, pharmacokinetics and Drug-likeness were all evaluated on the same webpage.

3. Results

3.1. Prepared Protein Structure of the RBD of SARS-CoV-2 (7EAM_1) for Molecular Docking

The protein structure for the receptor binding domain of SARS-CoV-2 was retrieved from the Protein Data Bank as shown in Fig. 1a. This structure was prepared and refined by the appropriate addition of hydrogen, removal of non-interacting water, modeling of missing loops and side chain, adding of relevant disulfide bond and minimizing the energy of the structure. The resultant output for the protein refinement is shown in Fig 1b.

Furthermore, the Ramachandran plot for the refined structure as shown in figure 1c, indicated that the refined protein structure has very minimized Ramachandran outliers and hence, it's an indication that its quality is acceptable for docking.

3.2. Predicting the Best Binding Site for Molecular Docking in the Protein Structure

After a global search around the processed structure using the sitemap tools of the Schrodinger suite v20.03, three (3) binding site was predicted together with its binding score, site score and pocket volume as shown in Table 1. Site 2 was selected because of its better score and highest volume. Figure 2 shows a grid generated around site, around which molecular docking analysis and screening was performed.

Table 1. The binding site with 7EAM_1 with their respective site scores and volume.

Site Number	Site Score	D-score	Volume
Site 1	0.682529	0.628868	94.325
Site 2	0.708399	0.585154	131.0260
Site 3	0.665813	0.647446	80.26200

3.3. Molecular Docking of the Ligand Library of Curcuma longa to the Protein Binding Pockets

A total of 50 different phytochemical ligands from the rhizome of Curcuma longa, which generated 266 conformations were docked against the binding pockets in the RBD of SARS-CoV-2 (7EAM_1). The docking scores and glide scores of the phytochemicals were compared to the score of the standard repurposed drug - Umifenovir (Arbidol). The phytochemicals with score higher than the standard repurposed drug were selected as a choice phytochemical for this study (Table 2 and Figure 3).

Table 2. Top potent phytochemical ligands from *Curcuma longa* with their Extra Precision docking score higher than the standard repurposed drug – Umifenovir (Arbidol).

	Phytochemical compounds	Entry ID	Canonical SMILES	Docking Score
1.	Quercetin	CID 5280343	<chem>C1=CC(=C(C=C1)C2=C(C(=O)C3=C(C=C(C=C3O2)O)O)O)O</chem>	-6.903
2.	1,7-Bis-(4-hydroxyphenyl)-1-heptene-3,5-dione (BHHD)	CID 9796708	<chem>C1=CC(=CC=C1CCC(=O)CC(=O)C=CC2=CC=C(C=C2)O)O</chem>	-4.349
3.	Cyclocurcumin	CID 69879809	<chem>COC1=C(C=CC(=C1)C=CC2=CC(=O)CC(O2)C3=CC(=C(C=C3)O)OC)O</chem>	-4.195
4.	<i>*Umifenovir (Arbidol)* - Standard</i>	CID 131411	<chem>CCOC(=O)C1=C(N(C2=CC(=C(C=C2)CN(C)C)O)Br)C)CSC3=CC=CC=C3</chem>	-4.176
5.	1,7-Bis-(4-hydroxy-3-methoxyphenyl)-1,4,6-heptatrien-3-one	CID 10904292	<chem>COC1=C(C=CC(=C1)C=CC=CC(=O)C=CC2=CC(=C(C=C2)O)O)O</chem>	-3.719
6.	Epi-procurcumenol	CID 10263440	<chem>CC1=CC(=O)C(=C(C)C)CC2C1CCC2(C)O</chem>	-3.719

3.6. Examining the Interactions of 1, 7-Bis-(4-hydroxyphenyl)-1-heptene-3, 5-dione with Amino-Acids residues in the Binding site of RBD of SARS-CoV-2

A number of interesting interaction was observed between 1,7-Bis-(4-hydroxyphenyl)-1-heptene-3, 5-dione (BHHD) in the binding pocket of the receptor binding domain (RBD) of SARS-COV-2 (Figure 4). Two hydrogen bonding was observed between the hydroxyl group of BHHD and ASN 437 and the carbonyl group of BHHD and TRP 436. Also, a pi-pi staking interaction was observed between the benzyl rings of BHHD and PHE 374 (Figure 4a). The 3D representation of the interaction showed that the molecule BHHD, is well fitted in the binding pocket of the receptor binding domain of SARS-CoV-2.

3.8. ADME/Tox Properties of 1,7-Bis-(4-hydroxyphenyl)-1-heptene-3,5-dione

The Adsorption, Distribution, Metabolism, Excretion and Toxicity (ADMET) profile of BHHD was predicted using the open source tools – SWISSADME. The value for all the parameters of the phytochemical properties, lipophilicity, water solubility, pharmacokinetics and drug-likeness falls within the non-toxic range and suitability it to be a lead molecule (Table 3)

Table 3. ADME/Tox Properties of 1,7-Bis-(4-hydroxyphenyl)-1-heptene-3,5-dione.

ADME/Tox	Parameter	Value
Physicochemical Properties	Formula	C ₁₉ H ₁₈ O ₄
	Molecular weight	310.34 g/mol
	Num. heavy atoms	23
	Num. arom. heavy atoms	12
	Num. rotatable bonds	7
	Num. H-bond acceptors	4
	Num. H-bond donors	2
Lipophilicity and water solubility	Topological PSA	74.60 Å ²
	Log <i>P</i> _{o/w} (iLOGP)	1.94
	Consensus Log <i>P</i> _{o/w}	2.88
Pharmacokinetics	H ₂ O solubility class	Moderately soluble
	GI absorption	High
	BBB permeant	Yes
Druglikeness	P-gp substrate	No
	Lipinski	Yes: 0 violation

Bioavailability score

0.55

4. Discussion

Highly pathogenic viruses such as SARS-CoV-2 pose a significant threat to human health, yet in most cases, therapies to prevent or treat these diseases are not yet optimum. The COVID-19 outbreak is an unprecedented global public health challenge and needs immediate intervention [6]. With the current threat looming all over the world, there is urgency to develop both effective diagnostics and newer therapeutics at an affordable cost with minimum or no side effect. Consequently, bioactive phytochemicals from plants which have been long used against several diseases, including other viral infections are now being considered as a therapeutic option [7]. *Curcuma longa* (Turmeric) amongst other therapeutic plants have been reported with potent antimicrobial and antiviral activities [8,9]. During the early onset of the COVID-19 pandemic, there were several social media jingles about the palliative and preventive effects of the decoction from the rhizome of turmeric against SARS-CoV-2 infections. More so, many people were reported to have gotten well from the COVID-19 symptom by just inhaling steams from the plant decoction [10,11]. This study aims to address the paucity of evidence on the efficacy of phytochemicals from turmeric against SARS-CoV-2 infections.

The non-ubiquitous bioactive phytochemicals present in the rhizome of *Curcuma longa* was retrieved from Dr. Duke's phytochemical and ethnobotanical databases. A total of 50 different phytochemical ligands, which generated 266 conformations, were docked against the binding pockets in the RBD of SARS-CoV-2 (7EAM_1). Prior to the docking experiment, the protein structure retrieved from the protein data bank (PDB ID: 7EAM_1) was preprocessed to reduce the probability of obtaining a false positive docking prediction. Although, there were no co-crystallized ligands which would have been used for the docking program validation, the library of phytochemical docking with a repurposed standard drug (Arbidol) which has been reported in literature to have anti-COVID activities by binding the RBD of the Spike protein of SARS-CoV-2. Other known repurposed drugs such as Hydroxyl-chloroquine, Remdesivir and Ritonavir would not have been suitable for the studies, as they target other proteins of SAR-CoV-2 rather than the receptor binding domain. A study conducted by Padhi et al. [12] reported that Arbidol binds suitably between the interface of the SARS-CoV-2 RBD and ACE2 receptors. Hence, the study concluded that the drug Arbidol will probably prevent viral entry into the host cells, from their molecular dynamic simulation experiment.

The docking scores and glide scores of the phytochemicals were compared to the score of the standard repurposed drug - Umifenovir (Arbidol). The phytochemicals with a score higher than the standard repurposed drug were Quercetin; **1,7-Bis-(4-hydroxyphenyl)-1-heptene-3,5-dione (BHHD)**; and Cyclocurcumin as reported in Table 2. This shows the possibilities of these phytochemicals to prevent viral entries in the host cells. Although Quercetin had the highest docking score, this study critically examined the interaction of 1,7-Bis-(4-hydroxyphenyl)-1-heptene-3,5-dione (BHHD) in the binding pocket of the receptor binding domain of SARS-CoV-2. Several studies have examined the interaction and the potency of Quercetin against SARS-CoV-2 [13]. More so, Quercetin is presently undergoing clinical trials [14–16], although the proposed mechanism of action reported was against SARS-CoV-2 protease.

The compound 1,7-Bis-(4-hydroxyphenyl)-1-heptene-3,5-dione (BHHD) showed significant binding affinity to the RBD of SARS-CoV-2 upon docking. The interaction in the binding pocket of the RBD of SARS-CoV-2 revealed BHHD to be a promising antagonist of the RBD of SARS-CoV-2. Two hydrogen bonding to two catalytic residues ASN 437 and TRP 436 in the binding pocket were captured in the 2D representation from Figure 4a. The pi-pi electron interactions between the benzyl of BHHD and PHE 374 indicate a stronger, more stable and more lasting binding. Studies have shown that asparagine 437, among glutamine, leucine, phenylalanine and serine are important residues in the receptor binding domain that enhances binding ACE2 of the host [17]. Also, Veeramachaneni et al.,

(202 discovered that residue 437-508 is very crucial for the binding of RBD to the Host ACE2. Another study, discovered an interaction with potency of corilagin with residues from Cys 336 to PHE 374. The *in silico* results of their study were further confirmed by the potency and binding of corilagin observed in HEK293 cells transfected with hACE2-EGFP. Therefore, the interaction of BHHD to RBD residues such as ASN 437 and Phe 374 is an indication of the possibility of BHHD to block the SARS-CoV-2 viral entry.

An examination of ADMET properties from SwissADME free open access web server (<http://www.swissadme.ch/>), 1,7-Bis-(4-hydroxyphenyl)-1-heptene-3,5-dione (BHHD) showed excellent physiochemical, lipophilicity, water solubility, pharmacokinetics and Drug-likeness properties. The physiochemical properties of BHHD from table 3, showed the molecular weight of BHHD to be 310.34 g/mol, 7 rotatable bonds, topological PSA of 74.60 Å², which were all suitable for a lead drug molecule. Furthermore, the result of the pharmacokinetics parameters, BHHD was shown to be very suitable for oral administration, as it was not a good substrate for p-glycoprotein and also exhibited very high gastrointestinal absorption. More so, it's not just that BHHD has excellent GI absorption, it's also able to permeate the blood brain barrier, as predicted from Boiled egg model. More so, the bioavailability score of 1,7-Bis-(4-hydroxyphenyl)-1-heptene-3,5-dione is 0.55. The bioavailability score is a measure of the rate and fraction of the initial dose of a drug that successfully reaches either the site of action or the bodily fluid domain from which the drug's intended targets have unimpeded access. Drugs given by other routes apart from intravenous routes have an absolute bioavailability of less than 1 and the dose of a drug is directly proportional to its bioavailability [18]. Hence, more evidence for the suitability of the drug orally.

The *logP* value or lipophilicity is a crucial parameter to understand the cell penetration behavior of a molecule through cell membranes. The *logP* value of 1,7-Bis-(4-hydroxyphenyl)-1-heptene-3,5-dione was less than 5. If *logP* value is more than 5, it suggests reduced absorption and less permeability due to greater molecular hydrophobicity [19]. Furthermore, for the Lipinski rule of five, there is no violation. This rule states that a compound is more likely to be membrane permeable and easily absorbed via passive diffusion in human intestine if it matches the following criteria $\log P \leq 5$; $MW \leq 500$; HBAs (O + N atom count) ≤ 10 and HBDs (OH + NH count) ≤ 5 . The Lipinski rule of five suggests that molecules whose properties fall outside such boundaries are less likely to be orally absorbed [20].

This is the first study to investigate the anti-COVID potential of BHHD against SARS-CoV-2. Studies have shown that the drug (BHHD) was first isolated from *Curcuma longa* and was used as a protection against beta amyloid in rat, with aims to discover drugs against Alzheimer's disease (Park and Kim, 2002). The better docking score and ADMET properties of BHHD when compared to the standard drug (Arbidol), confers it our choice as the lead phytochemical. This study suggests for future investigation into BHHD potency and probable toxicity both in *vitro* and *in vivo*, on cell lines and on animal models respectively

3.2. Figures, Tables and Schemes

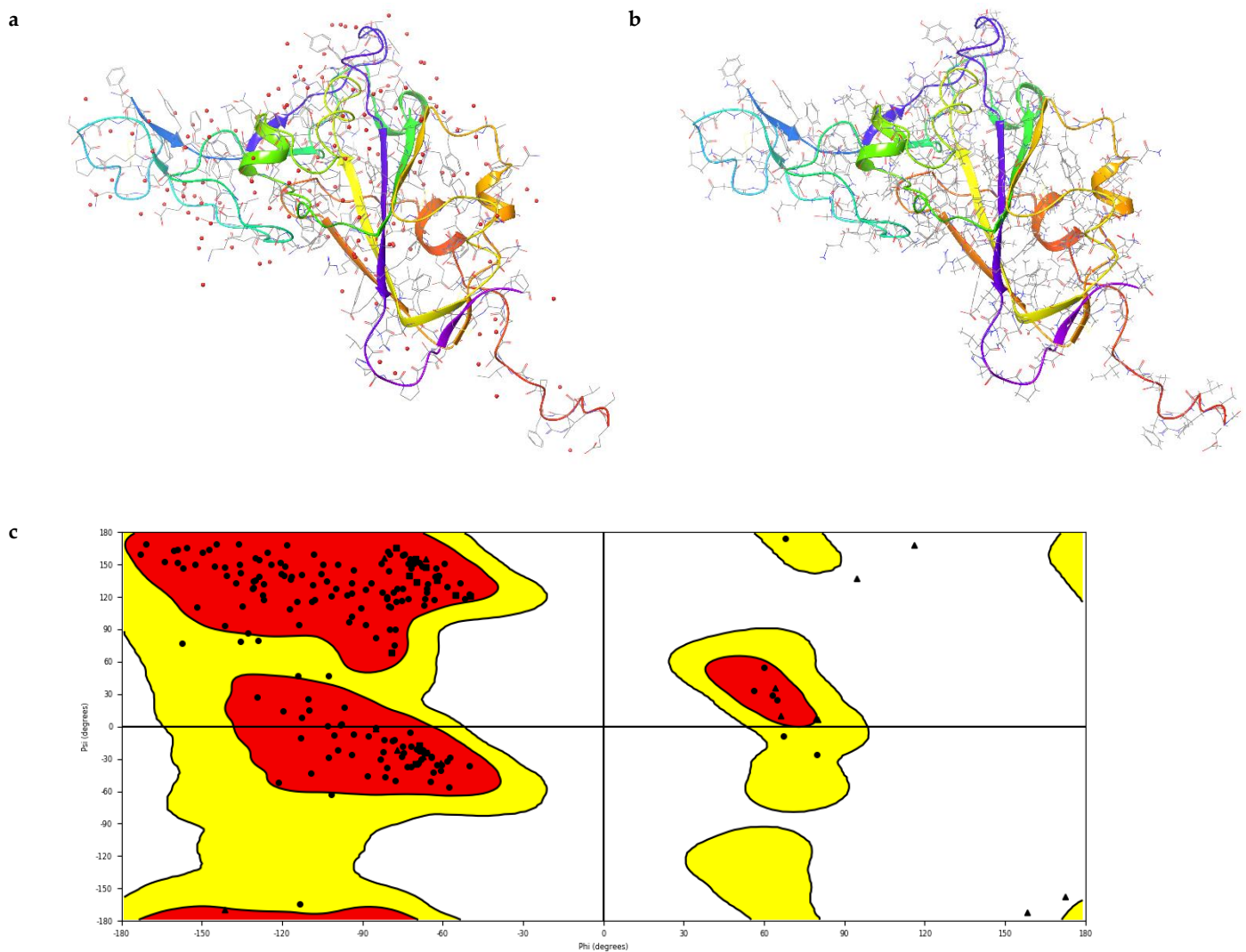


Figure 1. Processing the the protein structure of Receptor Binding Domain of the spike protein of SARS-CoV-2 (PDB ID: 7EAM_1). a) The unprocessed structure retrieved from Retrieved structure Protein Data Bank. (ID – 7EAM_1). The red dots represent the non-interacting water molecules. b) Structure after processing with the protein preparation wizard of Schrodinger suite. In this structure, the missing hydrogen have been added, non-interacting water molecules removed and energy of the crystal structure was minimised. c) Ramachandran plot for the processed structure of SARS-CoV-2. Each black dot represent an amino acid of the protein (7EAM_1). The black points in the red sector are best Ramachandran favored, the few dots in the yellow sector are good Ramachandran points while those on the white segment are the outliers. The processed structure is of high quality as it showed less than 1% outlier.

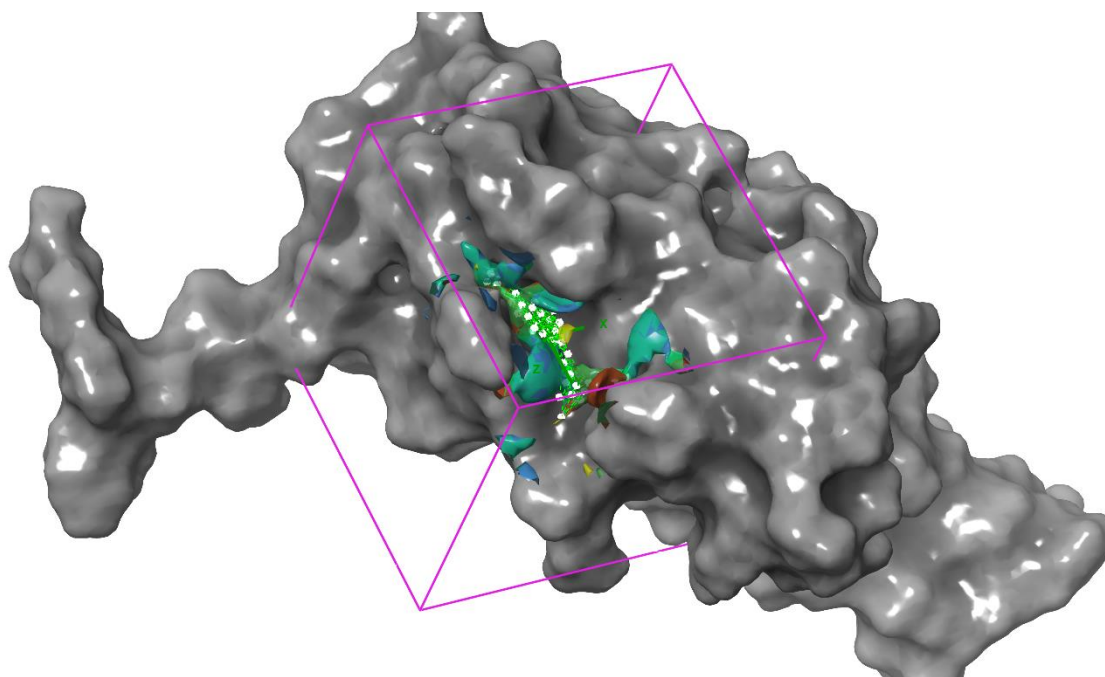


Figure 2. The surface representation of the RBD of SARS-CoV-2, with a purple grid box representing the perimeter around the binding site where ligands would be docked into. The red, blue, yellow and green patches represent the nature/property of the binding site 2. The red patch represents the hydrogen bond acceptor group, the blue patch represents the hydrogen bond donor groups, the green patch represents the hydrophilic region and the yellow patches are the hydrophobic regions.

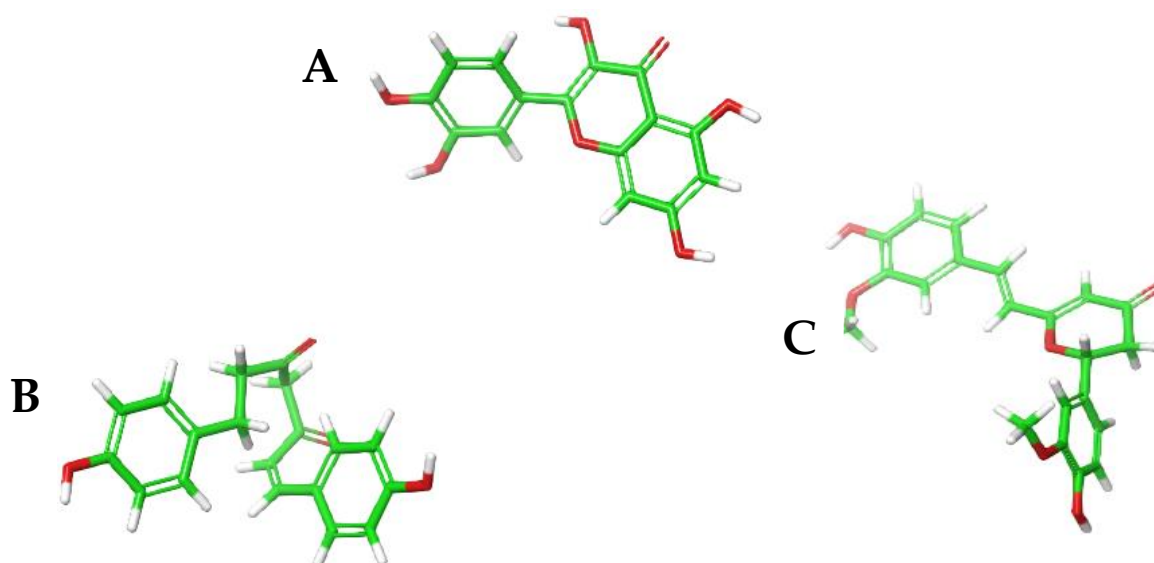
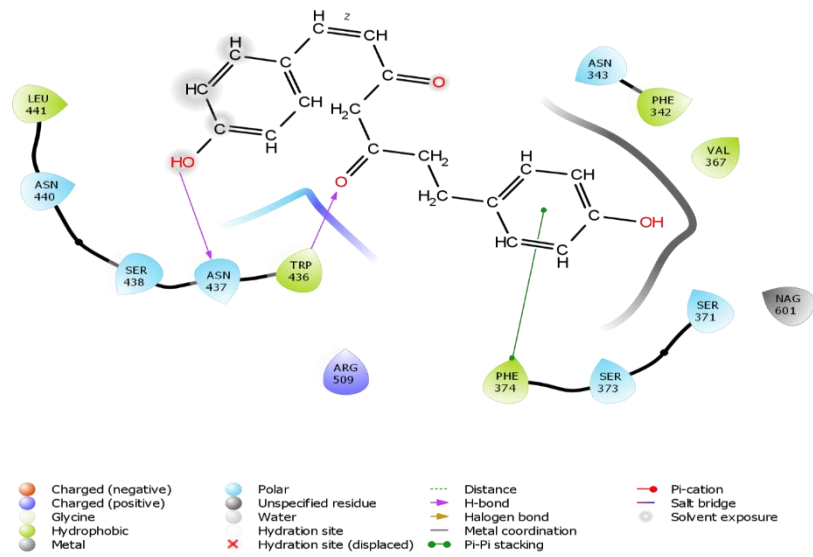


Figure 3. Three dimensional structures of the most potent phytochemicals from *Curcuma longa*, against the RBD of SARS-CoV-2. **A)** Quercetin (D-Score: -6.903) **B)** 1,7-Bis-(4-hydroxyphenyl)-1-heptene-3,5-dione (D-Score: -4.349) and **C)** Cyclocurcumin (D-Score: -4.195).

a



b

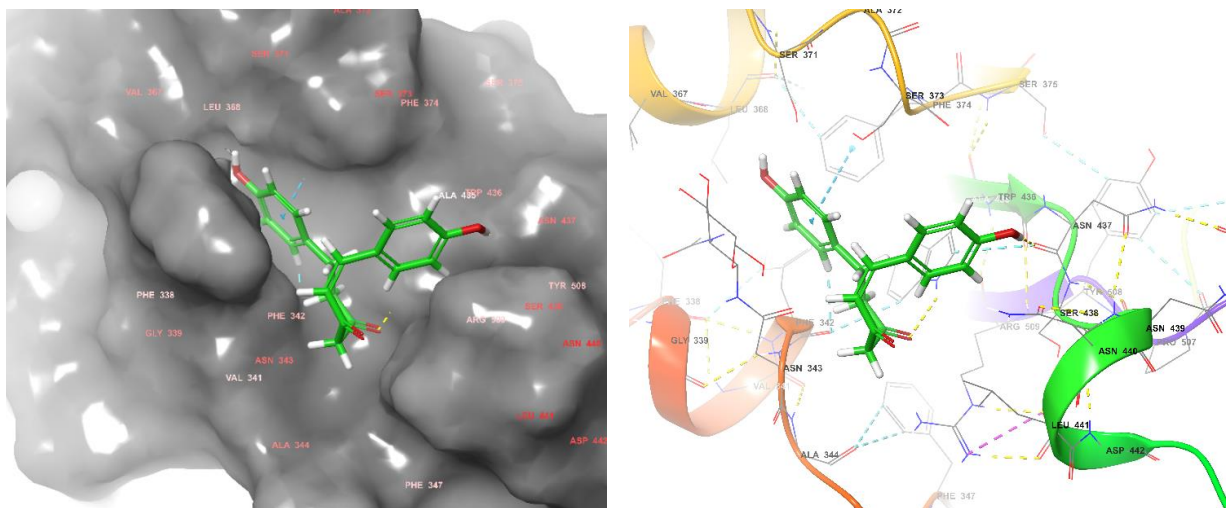


Figure 4. Interaction between the atom of 1,7-Bis-(4-hydroxyphenyl)-1-heptene- 3,5-dione (BHHD) and the amino acid residues of the binding pocket in the RBD of SARS-CoV-2. a) shows the 2D representation of BHHD in the binding pocket of RBD of SARS-CoV-2. b) Three Dimensional (Cartoon and Surface) representation of the **1, 7-Bis-(4-hydroxyphenyl)-1-heptene-3, 5-dione** in the binding pocket of RBD of SARS-CoV-2.

Author Contributions: For research articles with several authors, a short paragraph specifying their individual contributions must be provided. The following statements should be used “Conceptualization, T.P.C.E. and P.E.J.; methodology, N.O.U., P.O.O., M.C.O and C.K.O, software T.C.P.E. and R.O.A.; validation, T.C.P.E, E.J.N. and P. E. J.; formal analysis, T.P.C.E.; investigation, P.O.O., M.C.O and C.K.O.; resources, N.O.U and E.J.N.; data curation, T.C.P.E.; writing—original draft preparation, C.K.O., P.O.O and M.C.O; writing—review and editing, T.C.P.E. and C.K.O; visualization, T.C.P.E.; supervision, T.C.P.E, N.O.U and E.J.N.; project administration, P.E.J.

All authors have read and agreed to the published version of the manuscript.

Funding: This research received no external funding

Institutional Review Board Statement: Not applicable

Informed Consent Statement: Not applicable

Acknowledgments: In this section, you can acknowledge any support given which is not covered by the author contribution or funding sections. This may include administrative and technical support, or donations in kind (e.g., materials used for experiments).

Conflicts of Interest: The authors declare no conflict of interest.

References

1. Hu, B.; Guo, H.; Zhou, P.; Shi, Z.-L. Characteristics of SARS-CoV-2 and COVID-19. *Nat. Rev. Microbiol.* **2020**, *19*, 141–154, doi:10.1038/s41579-020-00459-7.
2. Lai, C.-C.; Shih, T.-P.; Ko, W.-C.; Tang, H.-J.; Hsueh, P.-R. Severe acute respiratory syndrome coronavirus 2 (SARS-CoV-2) and coronavirus disease-2019 (COVID-19): The epidemic and the challenges. *Int. J. Antimicrob. Agents* **2020**, *55*, 105924, doi:10.1016/j.ijantimicag.2020.105924.
3. Zhu, H.; Wei, L.; Niu, P. The novel coronavirus outbreak in Wuhan, China. *Glob. Heal. Res. Policy* **2020**, *5*, 1–3, doi:10.1186/S41256-020-00135-6.
4. L, D.; S, H.; J, G. Discovering drugs to treat coronavirus disease 2019 (COVID-19). *Drug Discov. Ther.* **2020**, *14*, 58–60, doi:10.5582/DDT.2020.01012.
5. M, I.; S, K.; NH, M.; Z, Z. Effect of the Phytochemical Agents against the SARS-CoV and Some of them Selected for Application to COVID-19: A Mini-Review. *Curr. Pharm. Biotechnol.* **2021**, *22*, 444–450, doi:10.2174/1389201021666200703201458.
6. Conti, P.; Caraffa, A.; Gallenga, C.E.; Kritas, S.K.; Frydas, I.; Younes, A.; Di Emidio, P.; Tetè, G.; Pregliasco, F.; Ronconi, G. The british variant of the new coronavirus-19 (Sars-cov-2) should not create a vaccine problem. *J. Biol. Regul. Homeost. Agents* **2021**, *35*, 1–4, doi:10.23812/21-3-E.
7. Ghildiyal, R.; Prakash, V.; Chaudhary, V.K.; Gupta, V.; Gabrani, R. Phytochemicals as Antiviral Agents: Recent Updates. *Plant-derived Bioact.* **2020**, *279*, doi:10.1007/978-981-15-1761-7_12.
8. Zorofchian Moghadamtousi, S.; Abdul Kadir, H.; Hassandarvish, P.; Tajik, H.; Abubakar, S.; Zandi, K. A review on antibacterial, antiviral, and antifungal activity of curcumin. *Biomed Res. Int.* **2014**, *2014*, doi:10.1155/2014/186864.
9. Parham, S.; Kharazi, A.Z.; Bakhsheshi-Rad, H.R.; Nur, H.; Ismail, A.F.; Sharif, S.; RamaKrishna, S.; Berto, F. Antioxidant, Antimicrobial and Antiviral Properties of Herbal Materials. *Antioxidants* **2020**, *Vol. 9*, Page 1309 **2020**, *9*, 1309, doi:10.3390/ANTIOX9121309.
10. Silveira, D.; Prieto-Garcia, J.M.; Boylan, F.; Estrada, O.; Fonseca-Bazzo, Y.M.; Jamal, C.M.; Magalhães, P.O.; Pereira, E.O.; Tomczyk, M.; Heinrich, M. COVID-19: Is There Evidence for the Use of Herbal Medicines as Adjuvant Symptomatic Therapy? *Front. Pharmacol.* **2020**, *11*, doi:10.3389/FPHAR.2020.581840.
11. Sahni; Sharma, H. Role of social media during the COVID-19 pandemic: Beneficial, destructive, or reconstructive? *Int. J. Acad. Med.* **2020**, *6*, 70, doi:10.4103/IJAM.IJAM_50_20.
12. Padhi, A.K.; Seal, A.; Khan, J.M.; Ahamed, M.; Tripathi, T. Unraveling the mechanism of arbidol binding and inhibition of SARS-CoV-2: Insights from atomistic simulations. *Eur. J. Pharmacol.* **2021**, *894*, 173836, doi:10.1016/j.ejphar.2020.173836.
13. Gu, Y.-Y.; Zhang, M.; Cen, H.; Wu, Y.-F.; Lu, Z.; Lu, F.; Liu, X.-S.; Lan, H.-Y. Quercetin as a potential treatment for COVID-19-induced acute kidney injury: Based on network pharmacology and molecular docking study. *PLoS One* **2021**, *16*, e0245209, doi:10.1371/JOURNAL.PONE.0245209.
14. Pierro, F. Di; Iqtadar, S.; Khan, A.; Mumtaz, S.U.; Chaudhry, M.M.; Bertuccioli, A.; Derosa, G.; Maffioli, P.; Togni, S.; Riva, A.; et al. <p>Potential Clinical Benefits of Quercetin in the Early Stage of COVID-19: Results of a Second, Pilot, Randomized, Controlled and Open-Label Clinical Trial</p>. *Int. J. Gen. Med.* **2021**, *14*, 2807–2816, doi:10.2147/IJGM.S318949.
15. Pierro, F. Di; Derosa, G.; Maffioli, P.; Bertuccioli, A.; Togni, S.; Riva, A.; Allegrini, P.; Khan, A.; Khan, S.; Khan, B.A.; et al. <p>Possible Therapeutic Effects of Adjuvant Quercetin Supplementation Against Early-Stage COVID-19 Infection: A Prospective, Randomized, Controlled, and Open-Label Study</p>. *Int. J. Gen. Med.* **2021**, *14*, 2359–2366, doi:10.2147/IJGM.S318720.
16. Quercetin In The Treatment Of SARS-COV 2 - Full Text View - ClinicalTrials.gov Available online: <https://clinicaltrials.gov/ct2/show/study/NCT04853199> (accessed on Aug 15, 2021).
17. Satarker, S.; Nampoothiri, M. Structural Proteins in Severe Acute Respiratory Syndrome Coronavirus-2. *Arch. Med. Res.* **2020**, *51*, 482, doi:10.1016/J.ARCD.2020.05.012.
18. Price, G.; Patel, D.A. Drug Bioavailability. *xPharm Compr. Pharmacol. Ref.* **2020**, 1–2.
19. Ditzinger, F.; Price, D.J.; Ilie, A.-R.; Köhl, N.J.; Jankovic, S.; Tsakiridou, G.; Aleandri, S.; Kalantzi, L.; Holm, R.; Nair, A.; et al. Lipophilicity and hydrophobicity considerations in bio-enabling oral formulations approaches – a PEARRL review. *J. Pharm. Pharmacol.* **2019**, *71*, 464–482, doi:10.1111/JPHP.12984.
20. Lipinski, C.; Lombardo, F.; Dominy, B.; Feeney, P. Experimental and computational approaches to estimate solubility and permeability in drug discovery and development settings. *Adv. Drug Deliv. Rev.* **2001**, *46*, 3–26, doi:10.1016/S0169-409X(00)00129-0.

